ISSN (Online): 2583-7052

International Journal of Advanced Trends in Engineering and Management (IJATEM)
Vol. 03(07), JULY 2024, pp. 13-27

Article Title: Advanced Controller System with Hybrid Renewable Sources Enabling Vehicle-To-Grid and Grid-To-Vehicle Operations

Advanced Controller System with Hybrid Renewable Sources Enabling Vehicle-To-Grid and Grid-To-Vehicle Operations

V. S. Vaisali[1,*], R. Anuja[2]

[*]PG Student, Arunachala College of Engineering for Women, Manavilai, Kanyakumari, vaisalivamini@gmail.com.

[2]Assistant Professor, Arunachala College of Engineering for Women, Manavilai, Kanyakumari, anujakrish84@gmail.com

ABSTRACT

Power demand is rising worldwide, forcing the search for an alternative source to solve the imminent power crisis, which is expected to be accomplished through the deployment of grid-synchronized electric vehicles (EV). Wind and solar energy are incorporated into this integration to those concerns. One smart grid innovation that permits energy exchange between the EV and the grid is vehicle to grid (V2G) technology. For the purpose of charging EVs, this research proposes employing hybrid energy. Here, the neighboring household's linear and non-linear demands are powered by the excess electricity from the photovoltaics (PV) panel, wind turbine, and AC generator that is utilized to charge the EV battery. Because of its dependability and independence from the real system model, a proportional-integral (PI) controller is used to maximize the DC voltage extracted from the PV panel. The improved DC voltage overall is a result of the SEPIC converter's improved DC output. Concurrently, an AC generator is incorporated into the system to supply extra power to the grid. An artificial neural network (ANN) controller is used to convert the power generated by the PV panel's Sepic conversion process into an improved output that is then converted to AC using a 3-phase Voltage Source Inverter (VSI). Harmonic components in the VSI output are corrected with an LC filter to ensure grid compatibility and safe current injection into the grid. This paper discusses the usage of a bidirectional converter to adjust the EV battery's voltage. MATLAB 2021a / Simulink software is used to simulate and validate the proposed approach.

Keywords: Electric vehicles (EV), Photovoltaic (PV), vehicle to grid (V2G), Voltage Source Inverter (VSI), SEPIC converter

1 Introduction

The widespread adoption of EVs is predicted to be prompted by the rise in pollution levels, which in turn releases greenhouse gas emissions and the ensuing phenomenon of global warming. Three key components comprises a microgrid: a diesel generator that serves as the main power source, a PV and wind farm combined to generate energy, and a V2G system that

International Journal of Advanced Trends in Engineering and Management (IJATEM)
Vol. 03(07), JULY 2024, pp. 13-27

Article Title: Advanced Controller System with Hybrid Renewable Sources Enabling Vehicle-To-Grid and Grid-To-Vehicle Operations

is located close to the microgrid's load [1]. By maintaining critical loads of an energy system during an islanding, coordinated V2G control schemes can boost resilience. By offering V2G services, EVs, which are dispersed and increasingly widespread local resources, will be vital in boosting resilience during islanding emergencies [2]. The AC-DC converter is used to convert ac voltage to dc voltage. The wind energy system still involves the generator, gearbox, wind turbine, and AC-DC converter. A wind turbine converts wind energy into rotating mechanical energy, while a generator converts the mechanical energy in the turbine shaft into electrical energy [3]. However, before connecting an AC source to a DC microgrid, it needs to be converted to DC, thus DC/AC converters are needed for normal AC loads [4]. Various MPPT approaches, such as perturb and observe (P and O), incremental conductance (INC), fuzzy logic controller (FLC), artificial neural network (ANN), and particle swarm optimization (PSO) algorithm, are employed to track the maximum power. The most popular MPPT methodology among these several approaches is P and O, MPPT, which has been proposed for PV system [5]. The PV through DC-DC boost converters are evaluated using several control strategies, including FLC, neural network, and, PSO for this improved settling point [6]. Because distributed energy resources (DERs) are situated close to the load, power transmission losses are additionally decreased. A DC microgrid is more power-efficient than AC. Easy-to-integrate energy storage technologies might provide lot of advantages [7]. DG resources in micro-grids are managed such that local loads are not significantly disrupted when they are disconnected and reconnected to the electric power supply. For the majority of DG solutions, converting the energy into grid compatible AC power necessitates a power electronics interface [8]. Energy Resource Management (ERM) in Microgrids is challenging due to the increasing use of unpredictable energy sources like solar PVs, Energy Storage Systems (ESSs), Demand Response (DR) programs, V2G or G2V, and electricity markets. All of these complications must be addressed while increasing revenue and decreasing total operational expenses for aggregators who collect all types of accessible energy resources from the Microgrid system. [9]. The primary characteristic of a four-port converter (FPC) is its capacity to handle energy sources with varying voltage and current properties. Throughout its operation, the proposed topology concurrently produce a buck and boost output. The converter is more dependable and economical when the FPC is implemented with a lower component count and a more straightforward control scheme [10].

The list below demonstrates how the paper is organised: Section I gives a description of the introduction. The recent works are described in Section II. The proposed model and description are explained in Part III. The results are presented in Section IV. In Section V, the conclusion is presented.

International Journal of Advanced Trends in Engineering and Management (IJATEM)
Vol. 03(07), JULY 2024, pp. 13-27

2 Recent Works

B. Chandrasekar et al [2020] [11] have presented a triple port converter that integrates a solar panel, battery, and DC load. It has two unidirectional and one bidirectional port. With a straightforward control technique, the proposed converter do both step-up and step-down conversions and has a positive high step-up/step-down output voltage. Nevertheless, there are more switches now, and there are difficulties implementing the digital controller.

H. M. Khalid et al [2020] [12] have analyzed the propagation and in-cell variation of a vehicle battery used in V2G technologies. The residual vector and hypothesis model provide support for the prediction structure, so improving the study of these fluctuations at the local level. Nevertheless, Li-ion battery packs are made up of hundreds of cells and it have complicated structure.

X. Zhu et al [2020] [13] have presented a high-boost voltage gain hybrid non-isolated active quasi-switched dc-dc converter that can be used for high step-up low power applications. Every capacitor has a capacitance value that is sufficient to keep the capacitor voltage constant. Nonetheless, the aforementioned boost-based non-isolated dc-dc converters have a broad, adjustable operational duty cycle range.

S. Wang et al [2020][14] have proposed a model for distribution network expansion planning that takes into account a variety of energy resource types on the distribution side. It is necessary to create multi-time period scenarios based on the charging probability state for each hour in order to create the scenario set of charging probability throughout a 24-hour period. The main drawback of the MCS-based strategy is that a significant number of samples must be generated, which could be computationally expensive, in order to attain a reasonable probabilistic distribution approximation accuracy.

A. Kulshreshtha et al [2020] [15] have presented a fourth-order boost dc-dc converter (FBDC) with minimum-phase response that exhibits continuous input and output current. In a low voltage low power dc distribution system (LVPDS), this converter is equipped with a voltage-mode controller to regulate bus voltage. Detailed research is necessary to determine how interactions resulting from the interconnection of bus regulating converters affect other converters that operate coherently.

3 Proposed Work Explanation

This novel grid tied EV charging system uses hybrid energy sources to connect the vehicle to the grid. A SEPIC converter is used to inject the ideal DC voltage that is derived from the PV panel using a PI controller, which aids in improvising the DC voltage. The necessary DC power is provided by a (PWM) rectifier in a wind energy conversion system based on a doubly fed induction generator (DFIG). After correct synchronization, a 3-phase VSI converts the power

International Journal of Advanced Trends in Engineering and Management (IJATEM)
Vol. 03(07), JULY 2024, pp. 13-27

output from the SEPIC converter and the improved output from the PWM rectifier into AC, which is then fed into the grid. The power output is kept in a DC link. Figure 1 presents the proposed system block diagram.

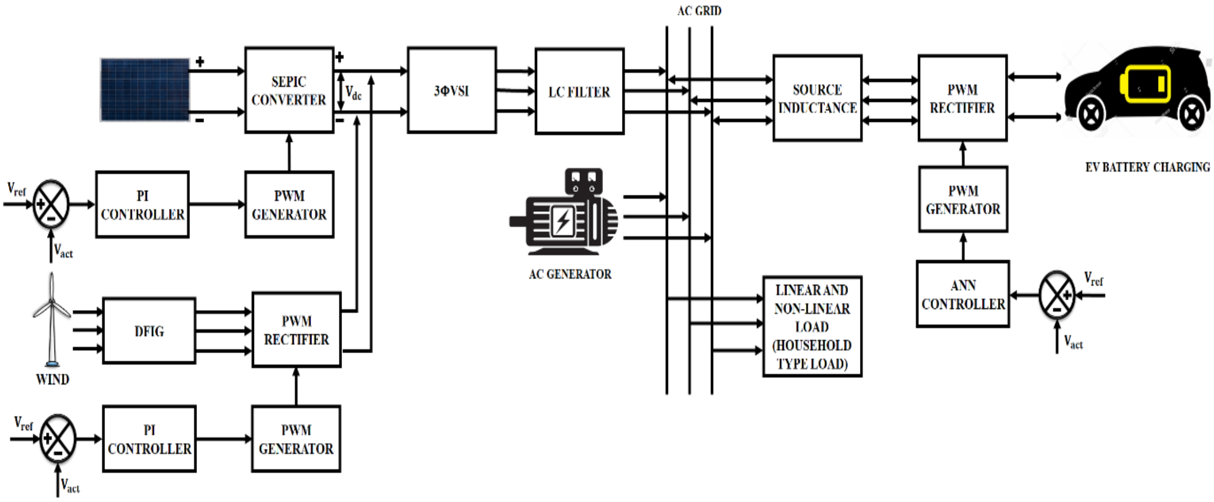

Figure 1: *Proposed block diagram*

An LC filter is used to rectify the harmonic present in the VSI, allowing the current to be safely injected into the grid. An EV's stored energy is effectively recycled back into the grid when it is not in use. The batteries of EVs are charged using electricity produced by photovoltaic cells, wind turbines, and AC generators. The excess energy is fed back into the grid for further applications, demonstrating two-way power transfer: Grid-to-Vehicle (G2V) and V2G. MATLAB 2021a/Simulink software is used to simulate and validate the suggested approach.

3.1 PV System

A tracking controller, power converters such as DC-DC converters and inverters, and several series and parallel combinations of PV modules comprise the PV system that is utilized for power conversion. Thus, a DC-DC converter is used to increase DC voltage produced, and an inverter is used to convert the DC voltage to AC. The PV panel needs to be chosen based on the load rating.

The electrical equivalent diode model of PV cell is shown in figure 2.

International Journal of Advanced Trends in Engineering and Management (IJATEM)
Vol. 03(07), JULY 2024, pp. 13-27

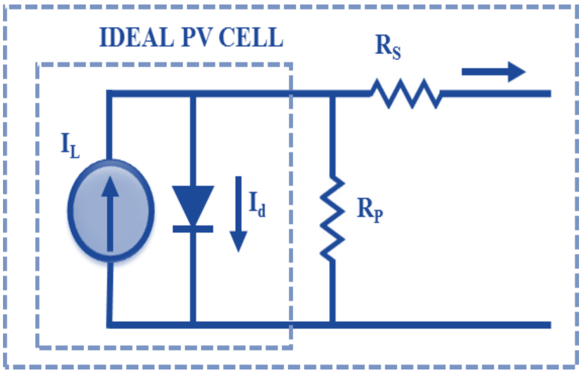

Figure 2: *Equivalent circuit of PV cell*

The PV model constitutes current sources, diode Shunt resistance R_{sh}, Series Resistance R_s. Shunt Resistance R_{sh} represent the cell surface leakage through the edges.

3.2 Wind Energy Conversion Systems

The purpose of wind energy conversion systems (WECS) is to transform wind energy into mechanical power. This mechanical energy is transformed into electrical by wind turbine generators, and it is utilized by windmills to power machinery, pump water, and grind grain. The rectifier is used to first convert the generator's variable output ac power into dc. The modulation index of the inverter is adjusted to feed the available dc power into the grid at the necessary constant voltage and frequency.

3.3 SEPIC Converter

A DC-DC converter with an output voltage that has the same polarity as the input is called a SEPIC converter. The circuit diagram for SEPIC converter is shown in figure 3.It is possible for the output voltage to equal, exceed, or be less than the input voltage. It consists of an active power switch, typically a MOSFET T, which is referred to ground and is regarded as an easy-to-drive switch. As seen in the image below, the converter also includes a diode D, two inductors, L_A and L_B, and two capacitors, $C_C$and C_0.

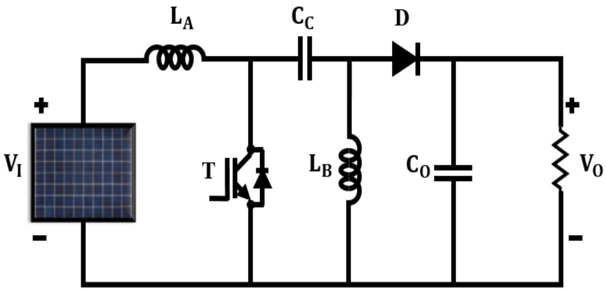

Figure 3: *SEPIC converter*

International Journal of Advanced Trends in Engineering and Management (IJATEM)
Vol. 03(07), JULY 2024, pp. 13-27

T ON condition

In this case, the voltages $V_i$and $V_C$are used to charge $L_A$and L_B, and switch T is activated. Due to the negative polarity of the coupling capacitorC_C, the diode D functions in reverse biased condition. Both $L_A$and L_B, are charged upon the coupling capacitor discharging. Figure 4 and 5 shows the circuit when the MOSFET is turned ON and OFF.

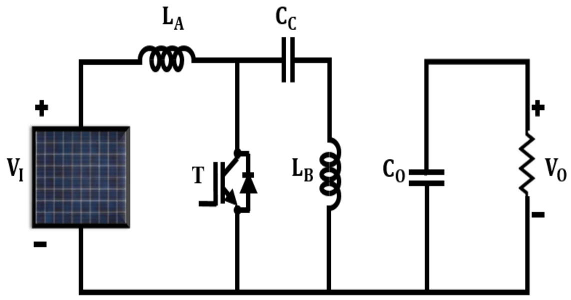

Figure 4: *T ON condition*

T OFF condition

The diode D is in a forward biased state in this instance. The energy from the inductor L_B is transferred to the output, while the coupling capacitor $C_C$is charged by the inductor L_A . The circuit schematic below shows the MOSFET in its turn-off state.

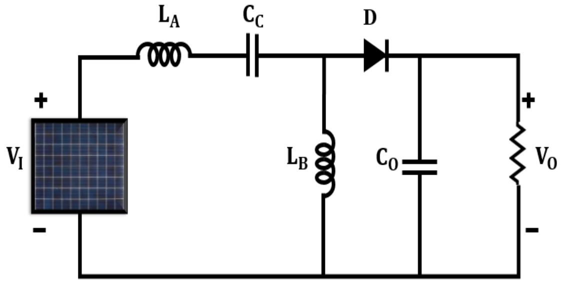

Figure 5: *T OFF condition*

The duty cycle of the SEPIC converter is given by,

$$D = \frac{V_o + V_D}{V_i + V_o + V_D} \tag{1.1}$$

Where V_i= input voltage
V_O= output voltage
V_d= diode voltage

The inductance values are given by,

International Journal of Advanced Trends in Engineering and Management (IJATEM)
Vol. 03(07), JULY 2024, pp. 13-27

$$L_A = L_B = \frac{V_{i(min)}}{\Delta I_L * fSW} \tag{1.2}$$

Where $V_{i(min)}$= minimum input voltage
The peak voltage of the MOSFET is given by,

$$V_P = V_i + V_o \tag{1.3}$$

The peak current of the MOSFET is given by,

$$P = I_{LAP} + I_{LBP} \tag{1.4}$$

Where I_{LAP} = peak current across L_A
I_{LBP} = peak current across L_B
The minimum peak reverse voltage of the diode is given by,

$$V_{PRD} = V_{i(\max)} + V_{o(\max)} \tag{1.5}$$

The rms current across the coupling capacitor is given by,

$$I_{Cc}(rms) = I_o \sqrt{\frac{V_O + V_D}{V_{i(max)}}} \tag{1.6}$$

The rms current across the output capacitor is given by,

$$I_o(rms) = I_o \sqrt{\frac{V_O + V_D}{V_{i(min)}}} \tag{1.7}$$

Compared with other traditional converters, the SEPIC converter achieves higher voltage gain and output power. Voltage gain increases in combination with duty ratio increases. With only one switch, the circuit maintains its simplicity and lower switching losses.

3.4 Three Phase Voltage Source Inverter

Two stage converters are used in rectifier fed inverter systems. Duty cycle is determined through the rectifier side control. Voltage control is necessary for the majority of inverter applications. Different criteria are used to categorize voltage source inverters. They are categorized based on how many phases they produce. As a result, inverters are classified as single-phase or three-phase based on the voltages they output.

3.5 LC Filter

First, the maximum ac current ripple needs to be determined to construct the LC filter. Using 5% of the phase current at rated power, the inverter side inductance is chosen in this configuration. This rule makes the assumption that the basic component of grid current is zero. Consequently, the filter inductor voltage's basic component also be zero.

International Journal of Advanced Trends in Engineering and Management (IJATEM)
Vol. 03(07), JULY 2024, pp. 13-27

Article Title: Advanced Controller System with Hybrid Renewable Sources Enabling Vehicle-To-Grid and Grid-To-Vehicle Operations

3.6 AC Generator

An AC generator's main function is to produce electricity for use in power plants for a variety of uses, from large-scale utility power generation to portable or small-scale home generators. Integral parts of power plants that provide electricity to the grid are AC generators. AC generators are employed in EVs as range extenders or to recharge the battery as necessary to increase the vehicle's operating range.

3.7 PWM Generator

Producing pulse width modulated gate pulse signals and feeding them to the converter's switch is the primary purpose of the PWM generator.

3.8 PWM Rectifier

The PWM Rectifier operates on the idea of force commutation techniques and is a regenerative converter. Since DC bus voltage is utilized in several applications, the converter's output, which is DC voltage in this case, should be constant. A control loop and DC capacitor are used to provide the constant DC bus voltage.

3.9 ANN controller for grid synchronization

Power systems employ an ANN based grid synchronization technology to produce accurately and efficiently synchronize renewable energy sources, such solar or wind power, with the utility grid. The input grid voltage and frequency are used by the ANN to calculate the control signal, or duty cycle, for PWM control. The power output of the renewable energy source is adjusted using this control signal to match the voltage and frequency of the grid.

4 Result and Discussion

The proposed work is implemented in MATLAB simulation and the following results are obtained. MATLAB/SIMULINK software is used to analyze the simulation results. High performance programming, visualization, and computation are all integrated in the user friendly MATLAB language for technical computing. Issues and their resolutions are stated using well-known mathematical notation. MATLAB is a high-level programming language and interactive environment utilized by millions of engineers and scientists across the world. The finest tool for signal analysis is MATLAB. Table 1 present the parameter specifications of the proposed work.

International Journal of Advanced Trends in Engineering and Management (IJATEM)
Vol. 03(07), JULY 2024, pp. 13-27

Table 1: Parameter specifications

PV and DFIG	
Parameters	Ratings
Open circuit Voltage	12V
Peak power	10Kw
Series connected Solar panel	36
Short circuit current	8.3A
No. of turbine	1
Voltage	575V
Switching frequency	10kHz
Power	10kW
SEPIC converter	
Switching Frequency	$10kHz$
$C_{a,}C_b$	$4.7\mu F$
L_a, L_b	$1\ mH$

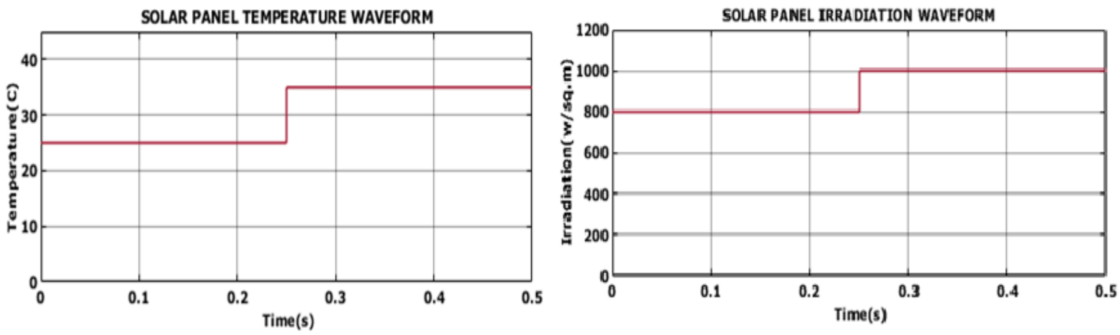

Figure 6: *Solar Panel Temperature waveform and Irradiation waveform*

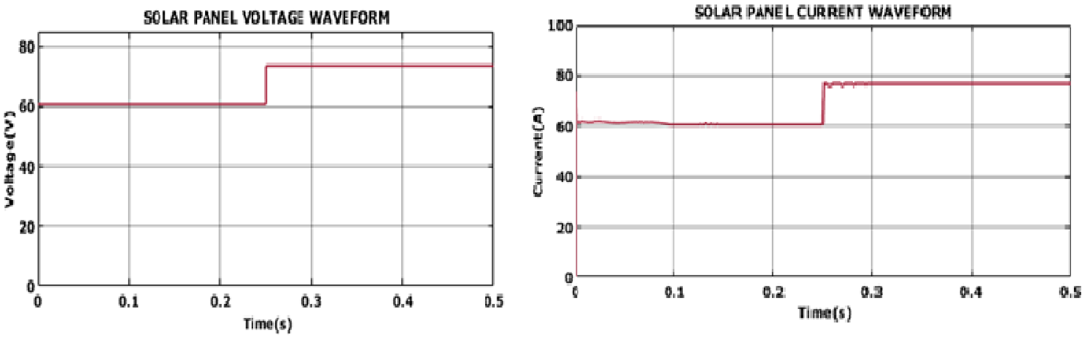

Figure 7: *Solar Panel Voltage waveform and Current waveform*

The temperature, irradiation, voltage, and current waveforms of the SEPIC converter are displayed in Figures 6 and 7. At 600 volts, the converter output value is finally attained. By

International Journal of Advanced Trends in Engineering and Management (IJATEM)
Vol. 03(07), JULY 2024, pp. 13-27

holding energy in an inductor and delivering it to the load at a higher voltage, this special capability is accomplished.

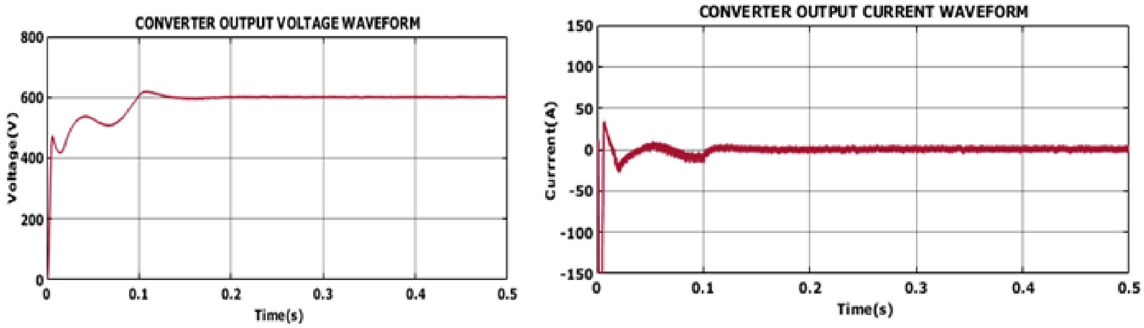

Figure 8: *Converter Output Voltage Waveform and Output Current Waveform*

Figure 8 shows the converter's voltage and current waveforms. When the voltage reaches its maximum or peak. It also shows that that when the voltage is at a maximum or peak, the current is also at a maximum or peak.

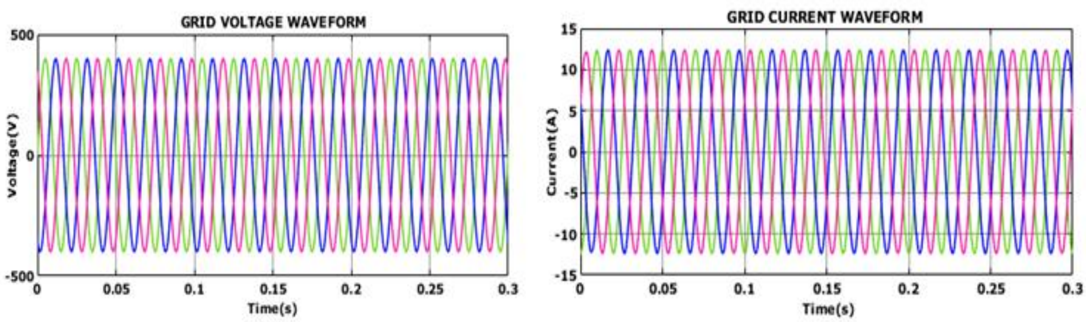

Figure 9: *Grid Voltage waveform and Grid Current waveform*

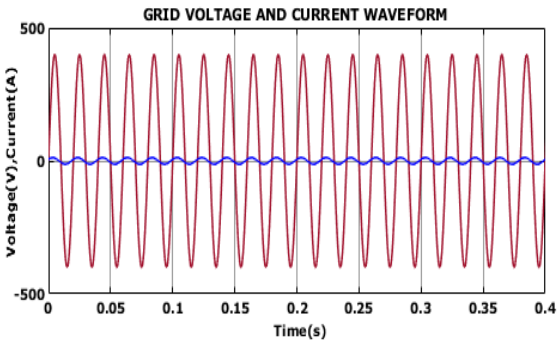

Figure 10: *Grid Voltage and Current waveform*

Figures 9 and 10 shows the output voltage and current waveforms for a sinusoidal grid with constant voltage and frequency.

ISSN (Online): 2583-7052

International Journal of Advanced Trends in Engineering and Management (IJATEM)
Vol. 03(07), JULY 2024, pp. 13-27

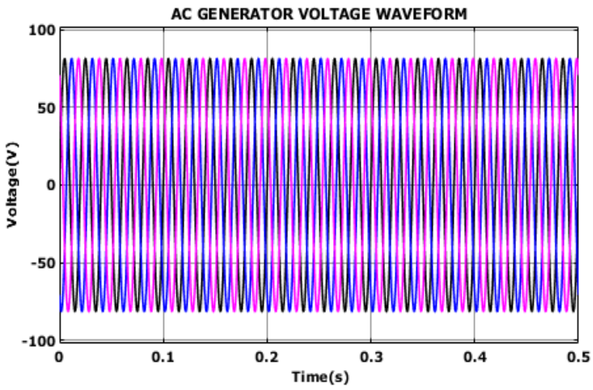

Figure 11: *AC Generator Voltage Waveform*

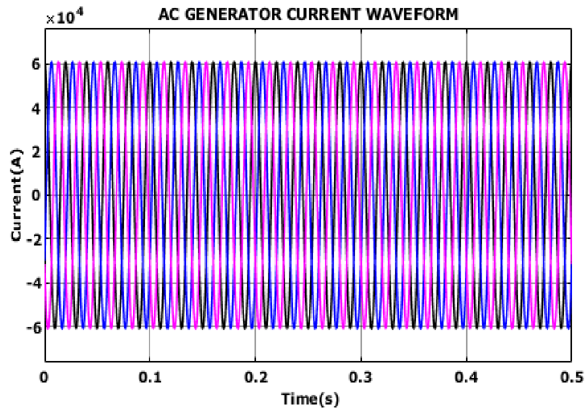

Figure 12: *AC Generator Current Waveform*

The voltage and current waveform of an AC generator is displayed in Figures 11 and 12. Faraday's law of electromagnetic induction, which states that electromotive force, often known as voltage, is generated when a current-carrying conductor cuts a uniform magnetic field, provides the basic theory for AC generators.

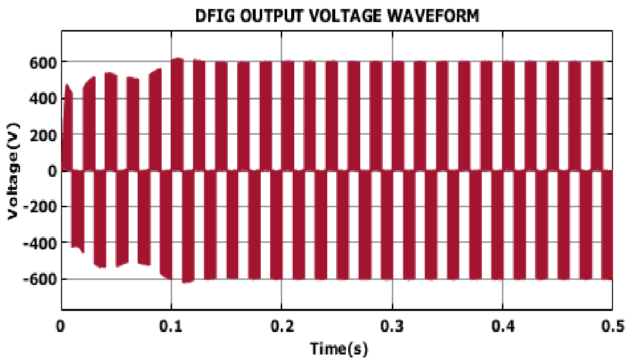

Figure 13: *DFIG Output Voltage Waveform*

International Journal of Advanced Trends in Engineering and Management (IJATEM)
Vol. 03(07), JULY 2024, pp. 13-27

The proposed WECS system's DFIG-based output voltage is displayed in Figure 13 and the voltage value is 600(V).

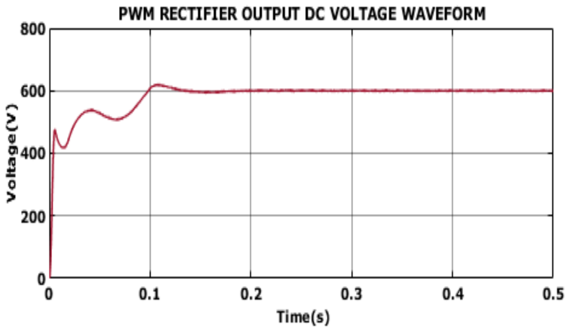

Figure 14: *PWM Rectifier Output DC Voltage Waveform*

Figure 14 illustrates how the PWM rectifier's output voltage is maintained at approximately 600 volts.

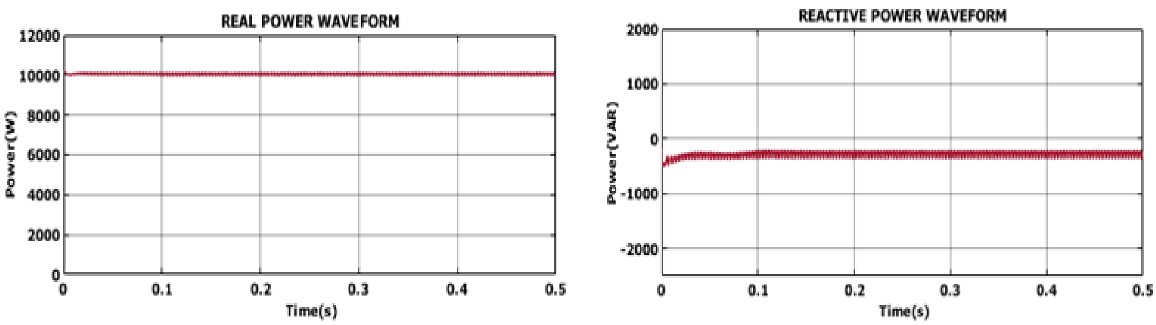

Figure 15: *Real Power waveform and Reactive Power Waveform*

The proposed work real and reactive power waveforms are displayed in Figure 15, with the real power reaching 10,000(W).

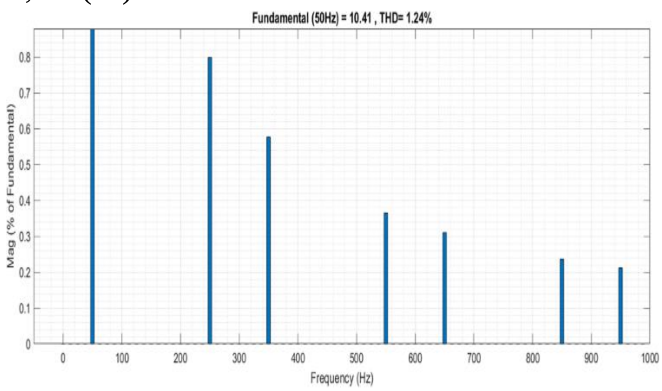

Figure 16: *THD Waveform*

International Journal of Advanced Trends in Engineering and Management (IJATEM)
Vol. 03(07), JULY 2024, pp. 13-27

The THD waveform, shown in figure 16, generates 1.24% grid current when an ANN controller is used for grid synchronization.

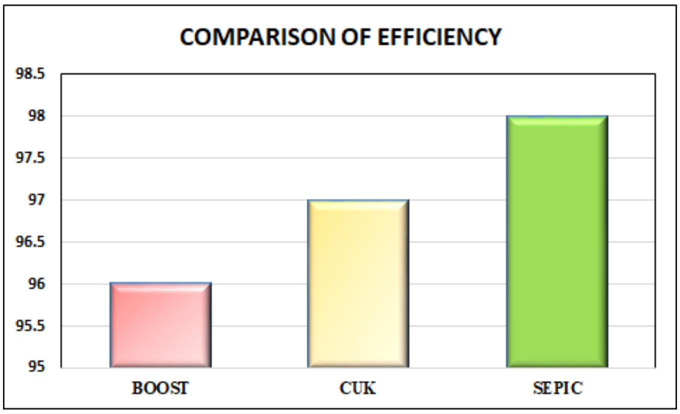

Figure 17: *Efficiency comparison*

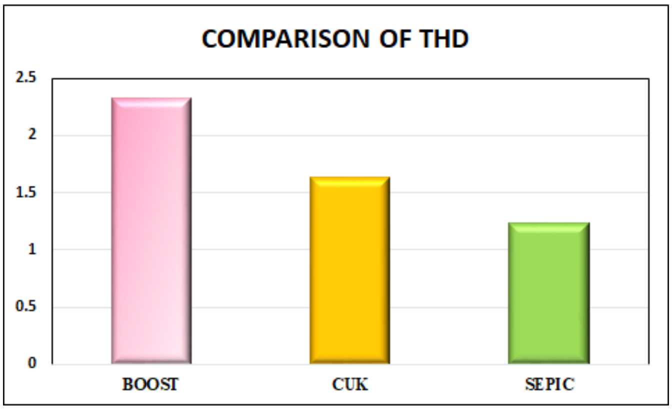

Figure 18: *Comparison of THD*

The efficiency and THD comparison is shown in Figures 17 and 18. The proposed SEPIC converter has a 98% efficiency rate and a 1.24% as total harmonic distortion.

5 Conclusion

In conclusion, this paper offered a novel solution to grid-tied electric car charging based on hybrid energy sources. It supports both grid-to-vehicle and vehicle-to-grid communications. The solar system feeds voltage to the inverter through a SEPIC converter. It is recommended that the SEPIC converter's current and the voltage of the DC bus be regulated using an energy management method. The WECS uses a PWM rectifier for DFIG and AC-DC conversion, which is controlled by a PI controller. A three-phase VSI is used to connect the converter's output, which converts the DC voltage into an AC voltage, to the grid. To produce sinusoidal

International Journal of Advanced Trends in Engineering and Management (IJATEM)
Vol. 03(07), JULY 2024, pp. 13-27

waveforms, the LC filter is employed to reduce harmonics. The PV panel, wind, and AC generator charge the electric vehicle battery, and any remaining power is used to power the next household's linear and nonlinear loads. During periods of low EV demand, the bidirectional power flow allows for effective charging of EV batteries as well as recycling surplus electricity back into the grid for other uses. Finally the hybrid charging technologies were successfully developed and considered to boost battery charging efficiency.

References

1. M. Abdelsattar, M. A. Ismeil, M. M. Aly and S. Saber Abu-Elwfa, "Analysis of Renewable Energy Sources and Electrical Vehicles Integration Into Microgrid," in *IEEE Access*, vol. 12, pp. 66822-66832, 2024, doi: 10.1109/ACCESS.2024.3399124.

2. L. Mauricette, Z. Dong, L. Zhang, X. Zhang, N. Zhang and G. Strbac, "Resilience Enhancement of Urban Energy Systems via Coordinated Vehicle-to-grid Control Strategies," in *CSEE Journal of Power and Energy Systems*, vol. 9, no. 2, pp. 433-443, March 2023, doi: 10.17775/CSEEJPES.2022.05270.

3. M. M. R. Ahmed *et al.*, "Mitigating Uncertainty Problems of Renewable Energy Resources Through Efficient Integration of Hybrid Solar PV/Wind Systems Into Power Networks," in *IEEE Access*, vol. 12, pp. 30311-30328, 2024, doi: 10.1109/ACCESS.2024.3370163.

4. R. V. Damodaran, H. Shareef, R. Errouissi and M. Eslami, "A Common Ground Four Quadrant Buck Converter for DC-AC Conversion," in *IEEE Access*, vol. 10, pp. 44855-44868, 2022, doi: 10.1109/ACCESS.2022.3169758.

5. H. Alhusseini, M. Niroomand and B. Mirzaeian Dehkordi, "A Fuzzy-Based Adaptive P&O MPPT Algorithm for PV Systems With Fast Tracking and Low Oscillations Under Rapidly Irradiance Change Conditions," in *IEEE Access*, vol. 12, pp. 84374-84386, 2024, doi: 10.1109/ACCESS.2024.3412848.

6. I. G. Zurbriggen and M. Ordonez, "PV Energy Harvesting Under Extremely Fast Changing Irradiance: State-Plane Direct MPPT," in *IEEE Transactions on Industrial Electronics*, vol. 66, no. 3, pp. 1852-1861, March 2019, doi: 10.1109/TIE.2018.2838115.

7. L. Strezoski, H. Padullaparti, F. Ding and M. Baggu, "Integration of Utility Distributed Energy Resource Management System and Aggregators for Evolving Distribution System Operators," in *Journal of Modern Power Systems and Clean Energy*, vol. 10, no. 2, pp. 277-285, March 2022, doi: 10.35833/MPCE.2021.000667.

8. G. Kou *et al.*, "Load Rejection Overvoltage of Utility-Scale Distributed Solar Generation," in *IEEE Transactions on Power Delivery*, vol. 35, no. 4, pp. 2113-2116, Aug. 2020, doi: 10.1109/TPWRD.2019.2951949.

ISSN (Online): 2583-7052

International Journal of Advanced Trends in Engineering and Management (IJATEM)
Vol. 03(07), JULY 2024, pp. 13-27

9. D. Dabhi and K. Pandya, "Enhanced Velocity Differential Evolutionary Particle Swarm Optimization for Optimal Scheduling of a Distributed Energy Resources With Uncertain Scenarios," in *IEEE Access*, vol. 8, pp. 27001-27017, 2020, doi: 10.1109/ACCESS.2020.2970236.

10. K. Suresh *et al*., "A Multifunctional Non-Isolated Dual Input-Dual Output Converter for Electric Vehicle Applications," in *IEEE Access*, vol. 9, pp. 64445-64460, 2021, doi: 10.1109/ACCESS.2021.3074581.

11. B. Chandrasekar et al., "Non-Isolated High-Gain Triple Port DC–DC Buck-Boost Converter With Positive Output Voltage for Photovoltaic Applications," in IEEE Access, vol. 8, pp. 113649-113666., 2020.

12. H. M. Khalid and J. C. -H. Peng,' "Bidirectional Charging in V2G Systems: An In-Cell Variation Analysis of Vehicle Batteries," in IEEE Systems Journal, vol. 14, no. 3, pp. 3665-3675. 2020.

13. X. Zhu, B. Zhang and K. Jin, "Hybrid Nonisolated Active Quasi-Switched DC-DC Converter for High Step-up Voltage Conversion Applications," in IEEE Access, vol. 8, pp. 222584-222598, 2020.

14. S. Wang, Z. Y. Dong, C. Chen, H. Fan and F. Luo, , "Expansion Planning of Active Distribution Networks With Multiple Distributed Energy Resources and EV Sharing System," in IEEE Transactions on Smart Grid, vol. 11, no. 1, pp. 602-611, 2020.

15. A. Kulshreshtha, A. R. Saxena and M. Veerachary, 2020, "Non-Isolated Fourth-Order Boost DC-DC Converter for Power Management in Low Voltage Low Power DC Grids: Design and Interaction Analysis," in IEEE Access, vol. 8, pp. 196500-196514.